Atomic Spectroscopy

Article

Molecular LIBS for Sorting and Analysis of Rare Earth Elements – Evaluation of Potential Applications

Michael Gaft *

Department of Physics, Ariel University, Israel

Received: *August 22, 2025;* ***Revised:*** *September 26, 2025;* ***Accepted:*** *September 30, 2025;* ***Available online:*** *September 30, 2025.*

DOI: 10.46770/AS.2025.149

ABSTRACT: The main purpose of this article is to attract attention to the molecular emission of rare earth elements (REEs) in laser-induced plasma (LIP) as a potential opportunity in addition to traditional atomic and ionic LIBS. This is relevant for analyzing REE-bearing materials of various types during exploration, mining, and processing. The first potential application is preliminary radiometric sorting, which enables the removal of a substantial portion of the waste rock from the entire technological process, making the development of even relatively low-grade deposits profitable. Additionally, products may be derived from the old waste, resulting in a positive ecological impact. Promising directions include electronic waste sorting, quantification of REE in Nd–Pr–Fe-B and Sm-Co super magnets, remote detection in nuclear-related applications, and the analysis of a small amount of a specific REE in the presence of a higher level of another one.

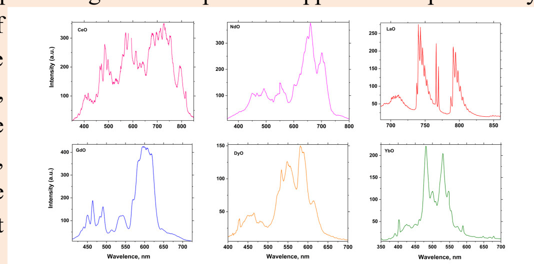

INTRODUCTION

Currently, rare earth elements (REEs) are considered Critical Elements or Strategic Materials, which are extremely important because they play an essential role in a wide range of consumer products, from smartphones to electric car motors, military jet engines, satellites, and lasers. Usually, new deposits of REE are relatively low-grade. In REE mining, only 0.1-0.5 g/t of the extracted materials are generally the valuable elements. Thus, most of the rock passes through the entire technological cycle to be transformed into waste, which not only fills the vast territories but also severely affects them. Additionally, significant amounts of energy and water are required for the extraction and processing of REEs from virgin rocks. Waste rock stockpiles contain radioactive elements, uranium, and thorium. Separating REEs from these radioactive elements results in health and environmental impacts, as well as increased processing costs. Open-pit mines, if exposed to rainwater, will pollute the environment with radioactive and toxic substances. Mine tailings also contribute to the negative environmental impacts of REEs in both the short and long term. Therefore, it can be concluded that REE mining, processing, and refining from alternative deposits entail substantial investment and environmental risks.[1-3]

The potential solution is electronic sensor-based sorting during the first stage before the primary technological process, when waste rock can be separated from the feed stream for further processing and is not unnecessarily ground. The electronic sensors detect mineral-specific absorption, emission, and reflectance under various electromagnetic waves, including radio, infrared, visible, ultraviolet, X-ray, and gamma rays, allowing for classification and separation based on chemical and physical properties.[4-7] Mineral sorting is based on the natural unevenness of the distribution of valuable components.

It is a physical process in which particles are separated based on their mineralogical composition. The objective of any beneficiation process is to separate the material being treated into two parts: a concentrate containing valuable minerals and a tailing containing non-valuable minerals. It enables the following advantages in comparison with existing methods: removing waste rocks, usually 70-80 % of the whole mass, for a fraction of the cost of treating through the complete process operation; decreasing mining efforts per one ton of product; decreasing of mineral resources loss; decreasing of costs using bulk excavation; additional valuable product extraction from ill-conditioned ore; decreasing of ore transportation expenses; less ecologically harmful excavation and ore process. The success of such a separation depends on two prerequisites: there should be sufficient differences in the physical properties of particles of different mineralogical compositions, and the valuable mineral to be enriched should be physically liberated from the gangue.

The first precondition relies on the selective feature typical of REE-bearing minerals, which do not exist in waste. It enables mineral identification during the time available for analysis on the conveyor moving belt.[4-6] Several sensor-based sorters were applied to ores containing rare earth elements (REEs). X-ray Transmission (XRT), suitable for any mineral with a density/atomic number difference between the desired component and the waste material, was the most effective. Reflectance spectroscopy can also be used to identify various rare earths. Neodymium exhibits some of the most pronounced absorption features among the REEs in the visible to Near-Infrared range at 580, 750, and 800 nm and can be used as a key pathfinder element for REEs. The absorption/reflection spectrum over multiple wavelength ranges is known as hyperspectral imaging, which appears suitable for sorting and remote sensing of rare earth elements.[7,8] The mineral's elemental composition is the best identification feature for REE-bearing minerals. LIBS is a potential approach for online elemental analysis and has gained popularity as a sorting technique.[9]

The second precondition for successful sorting is that valuable minerals should be physically liberated from waste. A concise and informative description of the mineralogical and elemental distribution of the drill core samples can aid in their evaluation. LIBS can offer a method for analyzing various types of mineral-based samples during mineral exploration, mining, and processing. Exploration is performed in field circumstances, and it would be cost-efficient to have a technique that could estimate the metal contents already in situ. It is essential in mining to reduce the amount of waste rock and ensure the mineralogical and chemical contents of the mineable ore units are already at the mine site. During mineral processing, it is essential to monitor the efficiency and quality of the processed mill and smelter products; an online analysis option would be an asset. LIBS offers an excellent choice for all these processes.[10-14]

Nevertheless, it is challenging to determine REEs by atomic and ionic LIBS in geological samples due to the relatively high detection limits and low concentrations typically encountered in most geological materials. Detecting trace amounts of REEs is even more difficult because their weak signals are often obscured by substantial interference from other major and minor elements in the rock matrix. Most REEs show only small intensity peaks in LIBS spectra of natural, unprocessed material under atmospheric conditions. So, a common approach is to use powder, pellets, or synthetic materials to detect or quantify the REE content or establish a theoretical Limit of Detection. The potential of molecular LIBS is often overlooked and does not currently apply to REE analysis, despite the existence of all relevant spectroscopic data.[15]

This paper is devoted to elucidating the potential application of REE molecular emission in LIP for the REE industry.

EXPERIMENTAL

The experimental setup is a conventional single-pulse (SP) LIP configuration (Fig. 1). A plasma plume is created by a laser pulse from an Nd-YAG 1064 nm laser (LQ215-D) with a pulse duration of 7 ns and an energy of 80 mJ per pulse. The laser beam is focused by a 20 cm focal lens, producing a perpendicularly incident beam with a diameter of approximately 600 µm at the surface. Accordingly, laser irradiance on the sample was approximately 30 J/cm^2. The sample was placed on a micrometric XYZ stage so that each laser shot impinged on a fresh portion of the sample surface. The emitted plasma radiation is collected by a fiber with a 0.22 numerical aperture and guided to two different spectrometers, depending on the research problem. The relatively broad, structureless molecular emission was analyzed using a Shamrock SR 303i-A spectrometer equipped with 300, 1200, and 2400 lines/mm diffraction gratings. For a spectrometer slit of 50 µm, the spectral resolutions are 0.1 nm for a 2400 l/mm grating, 0.16 nm for a 1200 l/mm grating, and 0.25 nm for a 300 l/mm grating. The detector is an intensified charge-coupled device camera (Andor DH-720 25F-03) with a time resolution of 5-6 ns. A precise delay generator, DG 645, synchronized the laser and the ICCD operations.

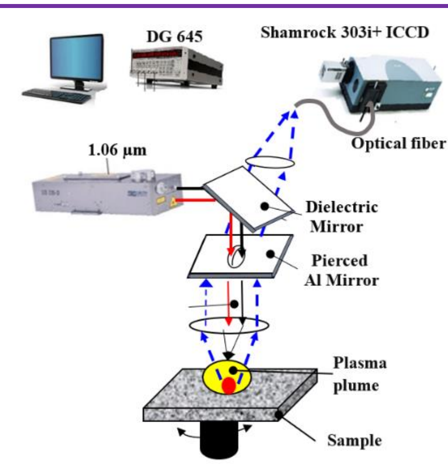

Fig. 1 Schematic representation of the laboratory experimental setup.

A ruggedized CCD spectrometer (Avantes AvaSpec) with a spectral resolution of 0.5 nm was used to evaluate the feasibility for industrial applications. It has a fixed integration time of 1 ms and a variable delay starting from 100 ns.

All spectra presented and analyzed in the manuscript are our original data. For molecular emission, acquisition delay D was 25-30 µs, and gate width W was 50-75 µs. Signals were averaged through 50-500 laser shots. The line intensities in the figures are presented in arbitrary units (a.u.); they may only be compared inside each figure, not between different figures.

The samples of the REE were prepared as pellets from corresponding chemically pure oxides (CeO_2, Nd_2O_3, Sm_2O_3, Gd_2O_3, Tb_2O_3, Dy_2O_3, Ho_2O_3, Er_2O_3, and Tm_2O_3, which are 99.9% pure; Pr_2O_3, Eu_2O_3, and Yb_2O_3, which are 99.99% pure). At such high levels of purity, the potential interference from the molecular emission of impurities is negligible. The pellets (13 mm diameter) were prepared by grinding (50–100 µm) under approximately 10 t of pressure for 60 s. Another sort of sample was rare-earth permanent magnets.

RESULTS AND DISCUSSION

LIBS as a distinctive feature. The REEs include scandium (Sc), yttrium (Y), lanthanum (La), cerium (Ce), praseodymium (Pr), neodymium (Nd), samarium (Sm), europium (Eu), gadolinium (Gd), terbium (Tb), dysprosium (Dy), holmium (Ho), erbium (Er), thulium (Tm), ytterbium (Yb), and lutetium (Lu). The most important industrial REE-bearing minerals are bastnasite $(Ce,La)CO_3F$, monazite $(Ce,La,Nd,Th)(PO_4,SiO_4)$, xenotime $Yb(PO_4)$, loparite $(Na,REE)_2Ti_2O$, and parisite $Ca(Ce,La)_2(CO_3)_3F_2$. Table S1 focuses on the primary atomic and ionic emission lines for the most significant REEs.[16] Besides REEs, a considerable number of accompanying elements are present, including magnesium (Mg), chromium (Cr), aluminum (Al), zirconium (Zr), manganese (Mn), niobium (Nb), tantalum (Ta), copper (Cu), zinc (Zn), silicon (Si), phosphorus (P), titanium (Ti), and iron (Fe) with multiple atomic and ionic emission lines.[17] Laser-induced plasmas are a highly transient and matrix-dependent emission source since the laser directly ablates the sample matrix. This situation differs significantly from the stable ICP plasmas and prepared ICP samples in a known solvent. The spectral complexity of such a complicated group of elements in REE-bearing rocks aggravates this situation. It limits the ability to accurately detect a suitable analytical line without spectral interferences. It requires high-resolution spectroscopy, knowledge of plasma conditions, and complex mathematical treatment.[18]

Online detection by molecular emissions may be preferred for the following reasons:

(1) Interfering atomic and ionic emissions have substantially shorter lifetimes in plasma than molecules and are extremely weak in a delayed plasma, where molecular emission remains strong.[5]

(2) Ionic and atomic emissions, especially those with resonance, are rarely used for the quantitative analysis of high-content samples due to the strong self-absorption effect. The molecular emission can potentially be a promising solution. For example, much lower self-absorption was found for BO than for B I and for BeO than for Be II.[19-21]

(3) The significant technological advantage of molecular emission is the relatively broad half-width of emission bands and their long plasma lifetime. Thus, we do not need high spectral resolution and a fine selection of delay and gate times. The long delay and broad gate are sufficient, and it is possible to use a relatively inexpensive CCD instead of the much more costly ICCD detectors.[22]

Nevertheless, in the absence of interfering atomic and ionic emission, molecular emission of accompanying elements may be present at such detection conditions, and its possible influence must be considered. The most abundant elements in Earth's crust with substantial molecular emissions in LIP are Fe, Mg, Al, and Ca. Thus, we must consider those elements, such as molecules with oxygen and fluorine, because several REE-bearing minerals contain F in their compositions. Besides, Ti is present in loparite and has molecular emission in LIP. An additional possibility is the presence of carbon with intense CN molecular emission (Fig. 2, Table S2 [22]).

Another emission source in LIP, which occurs after a very long delay, is Plasma-Induced Luminescence (PIL), which is observed in luminescent minerals such as fluorite, apatite, calcite, and zircon. For REE molecular identification, their influence combines spectral interference from transition metal luminescence with valuable information from trivalent REE luminescence, which exhibits forbidden electron transitions with long decay times and retains strong luminescence after a long delay in LIBS (Fig. 3).[23-24] Divalent REEs are characterized by allowed electronic transitions and are already quenched after a long delay time.[5] PIL is detected in the time window of molecular emission. The PIL of REE is a useful diagnostic feature together with the molecular spectrum, while the PIL of Mn^{2+} and Fe^{3+} interferes with molecular emission and may prevent REE identification.

Potential application in the mining industry. The intensity of molecular emissions is typically lower than that of corresponding atoms and ions (except for halogens).[25] Based on our accumulated experience, the minimum concentration for online LIBS analysis by molecular REE emission is 0.1 %. Thus, LIBS sorting may be effective for REE-bearing ores, coal, coal ash, and phosphorites.[1-2]. Fig. 4 presents the molecular emissions of Ce, La, Nd, and Yb,

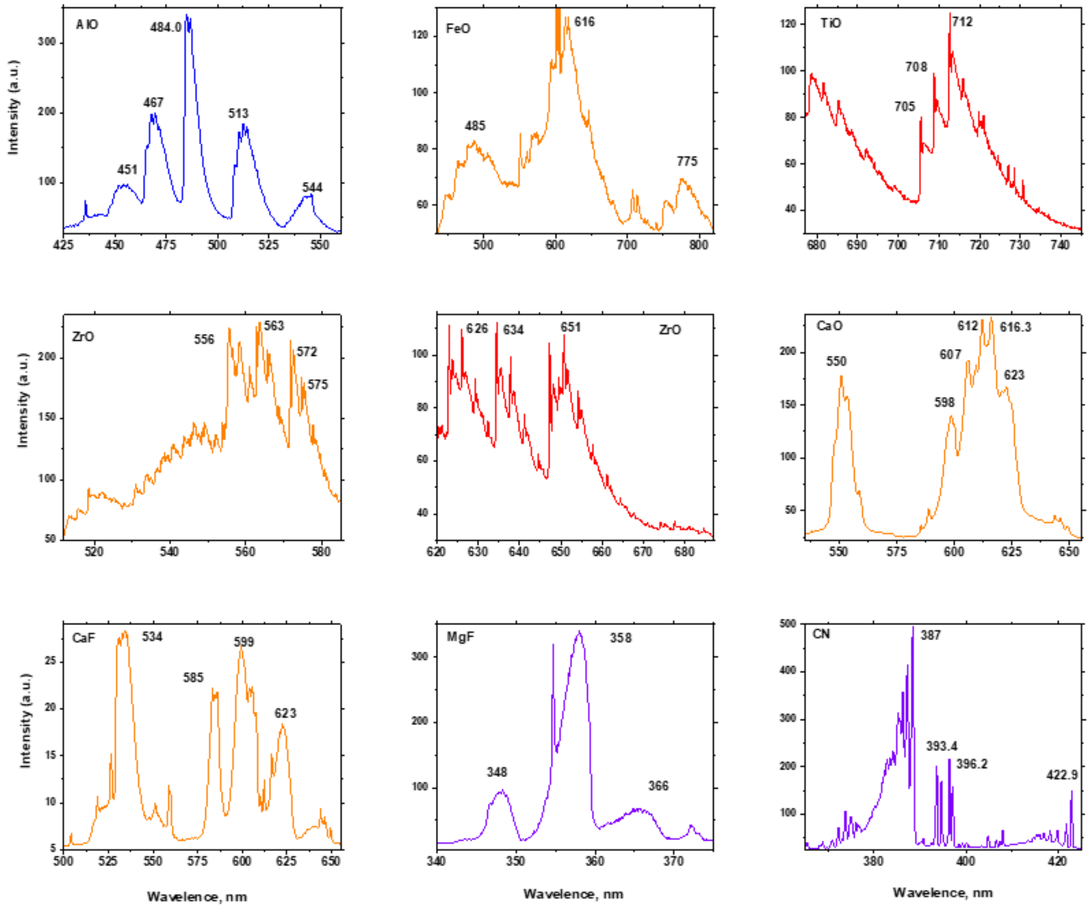

Fig. 2 Molecular emission spectra of the relevant accompanying elements in LIP: AlO, FeO, CaO, CaF, MgF, TiO, ZrO, and CN.

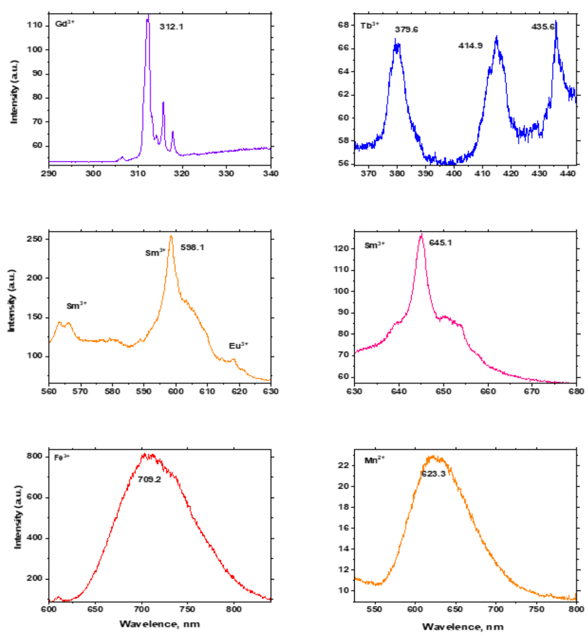

Fig. 3 Plasma Induced Luminescence of trivalent REE and Mn^{2+} and Fe^{3+} with long luminescence decay times.

which are most important for the mining industry. The selection of atomic or molecular LIBS as a distinctive feature is relevant to a specific mineralogic situation. In some instances, atomic emission lines can solve the REE-related task.[26] In other cases, for example, detecting La with atomic LIBS produces poor results in geological samples and may only be used after complex mathematical processing.[27] Applying atomic LIBS for detecting REEs in Fe-Mn concretions is also challenging due to significant spectral interferences and the generally low REE content. At the same time, the molecular emission of LaO is significantly more effective.[28]

The most recent publication considers the quantification of La, Ce, and Nd in rare-earth ores using LIBS. Due to the complex elemental composition of the samples, characterized by a high content of elements such as Si, Al, Fe, K, Ca, and Na in the matrix, the original spectra exhibit numerous spectral lines with significant spectral interference. As a result, the detected atomic and ionic peaks are difficult to identify as characteristic lines of specific elements due to spectral overlap. Even after employing the univariate analysis method, accurately selecting the characteristic lines of rare earth elements La, Ce, and Nd remains challenging because these elements exhibit numerous spectral

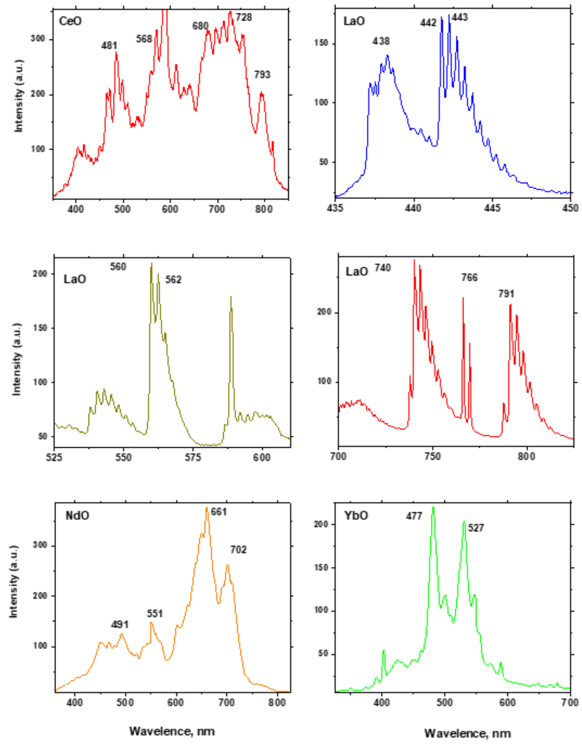

Fig. 4 Molecular emission spectra of the industrially relevant REE in LIP: CeO, LaO, NdO, and YbO.

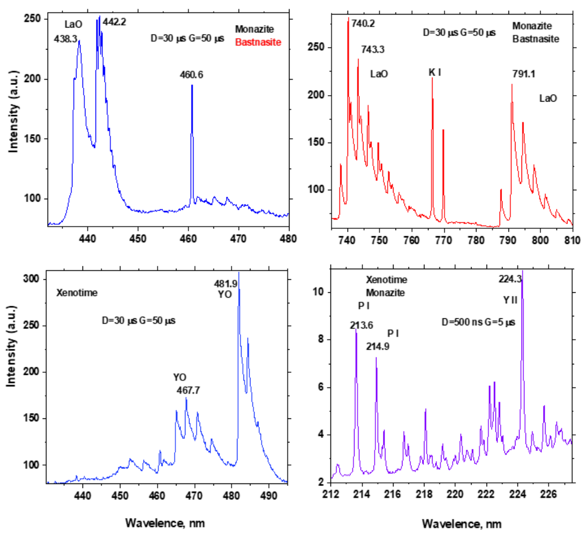

Fig. 5 Molecular and atomic LIBS of monazite, xenotime, and bastnasite allow their identification.

lines and are susceptible to substantial interference from matrix elements and spectral overlap among the rare earth elements.[29]

When solving this task using molecular LIBS, the influence of Si, K, and Na is negligible because their molecular intensities are very weak. The remaining major elements, Al, Ca, and Fe, generate intensive molecular bands. However, La, Nd, and Ce may still be detected in specific spectral windows: LaO by all three of its spectral series (blue, yellow, and red), while NdO and CeO are detected by their emissions in the 630-750 nm spectral range (Fig. S1).

Besides a good, distinctive signal, the second precondition for successful sorting is that valuable minerals should be physically liberated from waste. LIBS enables the evaluation of this precondition already in situ. REEs leaching and recovery processes depend on the mineralogical composition and morphological distribution of crystals containing different REEs. Rapid determination, imaging, and rough quantitative evaluation of those minerals enable their efficient exploration and recovery, reducing the amount of waste rock and ensuring the mineralogical and chemical contents of the minable ore units at the mine site. For example, the Raman mapping of REE-bearing minerals demonstrated the significant impact of REE distribution on beneficiation efficiency.[30] Mapping of REEs by molecular LIBS is much more sensitive than the inherently weak Raman signal.[31]

For example, accurately estimating the content of significant minerals containing REE (*e.g.*, xenotime, monazite, and bastnäsite) is crucial for efficiently extracting metal REEs from mines with REE reserves.[32] Using different elemental compositions of those minerals, the identification can be achieved relatively quickly through a combination of molecular and atomic/ionic LIBS. By molecular LIBS, the difference between xenotime YPO_4 and monazite $(Ce,La,Nd,Th)PO_4$, and bastnaesite $(Ce,La)CO_3F$ is straightforward because the spectra of YO and LaO are significantly different. The differentiation between bastnaesite and monazite is based on P I atomic lines, which are absent in bastnaesite (Fig. 5).

Recycling and analysis of REE-magnets and electronic waste. Fig. 6 presents REE molecular emission spectra in LIP for the most essential elements for NdFeB magnets sorting and analysis. End-of-life NdFeB magnets contain the highest amount of recyclable LREEs. There is enormous potential for recycling Nd from the end-of-life NdFeB magnets found in computer hard disk drives, as approximately 600 million are produced annually.[33,34] The applicability of atomic and ionic LIBS to the real-time analysis of commercial-grade B-Fe-Nd magnets was studied. It was demonstrated that LIBS has significant potential application as a rapid, accurate, inexpensive analytical technique for identifying rare-earth components commonly found in electronic devices. The lines at 406.93, 430.36, and 495.48 nm, relatively free from Fe emission interference, were used for Nd identification.[35] A quantitative analysis of Dy in coated NdFeB used magnets by laser-induced breakdown spectroscopy for sorting before recycling was recently proposed, utilizing atomic emission spectroscopy of Dy.[36] Besides Nd, the presence of Gd strongly influences the magnetic properties of rare-earth magnets. For Gd identification, the line at 432.55 nm was used.[37,38]

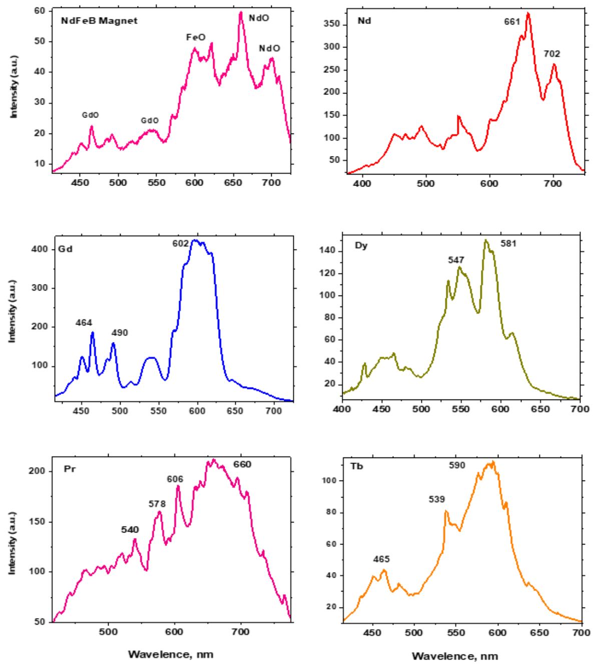

Fig. 6 Molecular emission of Nd-Fe-B Magnets and the reference spectra of its individual REE components.

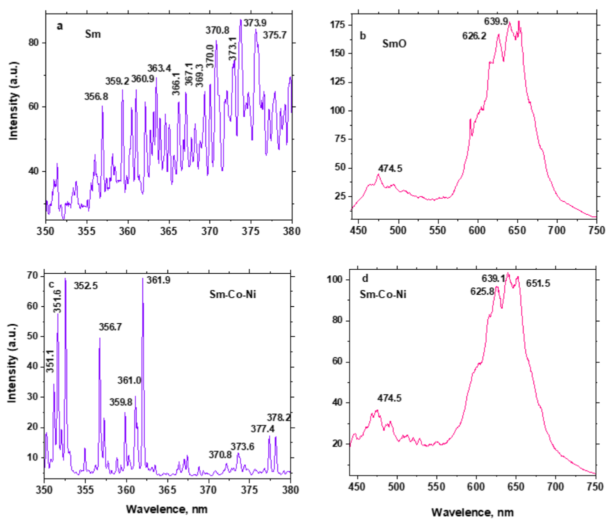

Fig. 7 Atomic and molecular emission of Sm and SmO in metallic Sm (a, b) and Sm-Co-Ni magnet (c,d).

Nevertheless, molecular emission appears to be more effective for the identification of Gd and Dy in mixtures with other REEs.[15]

A similar situation exists for Sm-Co magnets, where lines for Sm are challenging to detect within a complex matrix.[35] Fig. 7 presents our reference ionic and molecular Sm emission data in Sm-Co-Ni magnets. The comparison of ionic spectra for pure Sm and Sm-Co-Ni magnet reveals that the lines of Sm are extremely weak, while only the lines of Ni and Co are present. At the same time, such a matrix is optimal for SmO molecular emission detection because the significant elements Co and Ni are not characterized by appreciable molecular emission in LIP, and the SmO band is easily seen (Figs. 7b and 7d).

Besides magnets, other rare-earth-containing electronic devices are essential for sorting, including smartphones, digital cameras, computer hard drives, fluorescent and light-emitting diode (LED) lights, flat-screen televisions, computer monitors, and electronic displays. The most abundant REEs here are Ce (electrodes, catalytic converters), Nd (IR lasers), La (telescope lenses and IR absorbent glass), Dy (lasers), Tb (additive in rare-earth magnets), Ho (powerful magnetic properties), Sc (televisions and energy-saving lamps), and Y (superconductors, lasers).

Besides magnets, other rare-earth-containing electronic devices are essential for sorting, including smartphones, digital cameras, computer hard drives, fluorescent and light-emitting diode (LED) lights, flat-screen televisions, computer monitors, and electronic displays. The most abundant REEs here are Ce (electrodes, catalytic converters), Nd (IR lasers), La (telescope lenses and IR absorbent glass), Dy (lasers), Tb (additive in rare-earth magnets) (the spectra may be found on the Figures above), Ho (powerful magnetic properties), Sc (televisions and energy-saving lamps), and Y (superconductors, lasers) (Fig. 8).

A small amount of a certain REE in the presence of a higher level of another one. A good example is ceria (CeO_2) doped with low-valence rare-earth cations, such as Gd^{3+}. LIBS proposed a stoichiometric analysis, but the lanthanide elements emit numerous lines, making it challenging to identify a well-resolved single emission line of the dopants, even at 10% of Gd.[39] It was found that using the emission line at 462.0 nm, the molecular band of GdO is detectable even at 2 % Gd. Recently, ceria doped with Sm and Gd ions has been found to show better ion mobility than ceria doped only with Gd. The three lanthanide elements, which produced numerous emission lines, made it rare to identify well-resolved single emission lines of the dopants (Sm and Gd) without mathematical treatment.[40] Molecular emission presents better spectra for quantitative analysis (Fig. 9).

REE detection in the nuclear industry. LIBS has been considered a potential tool for completing specific measurements in the nuclear industry due to its rapid analysis, lack of sample preparation, remote measurement ability, and simultaneous multi-element analysis capability. One of the tasks is in-situ molten salt KCl-LiCl analysis, which has significant potential for use as next-generation nuclear reactor coolants and in pyro-processing for the recycling of used nuclear fuel. However, the molten salt composition must always be known, and high temperatures and intense ionizing radiation pose challenges for monitoring instrumentation. Atomic LIBS was applied to detect Pr, Eu, and Er.[41] However, molecular emission (Fig. 10) appears to be more

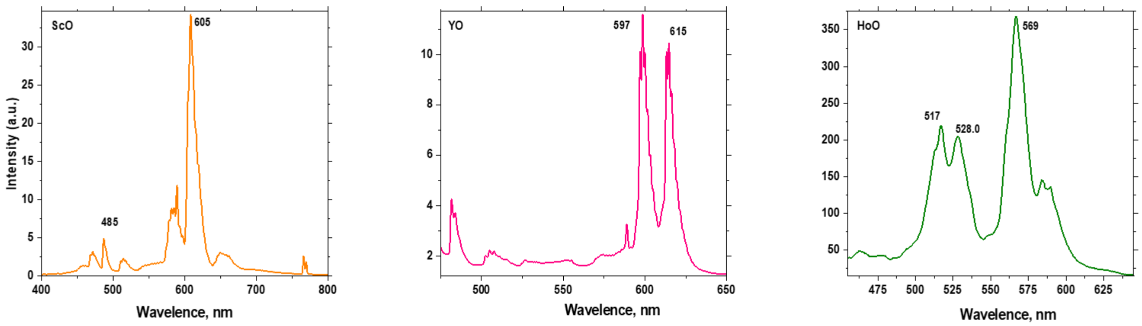

Fig. 8 Molecular emission spectra of the REEs relevant for electronic waste sorting: HoO, YO, ScO.

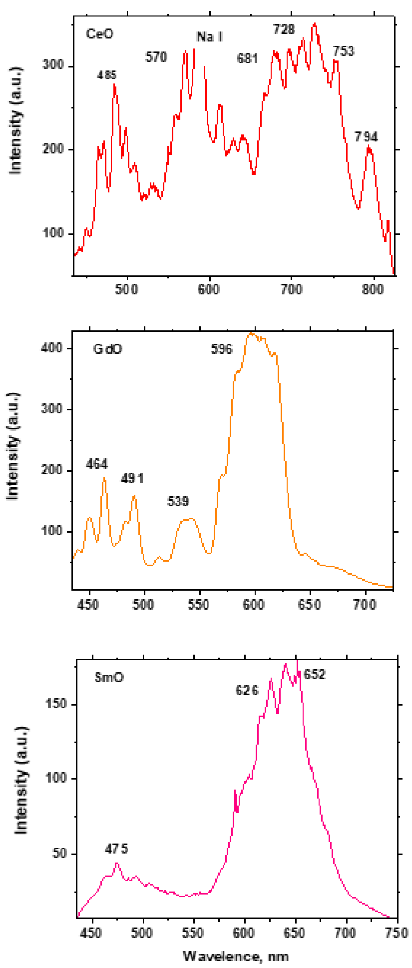

Fig. 9 Molecular emissions of the GdO and SmO relevant for analysis of Sm and Gd impurities in CeO_2.

preferential, as matrix elements K and Li do not exhibit molecular spectra. A similar situation occurs in the remote Gd analysis in the Th oxide matrix, where the characteristic emission lines of Gd in the complex spectra were reported at 348.12, 348.18, and 348.26 nm and were utilized for quantitative analysis. The strong background of the lines of Th makes the atomic Gd emission challenging to detect.[42] Molecular emission of GdO may be considered for this task because the matrix Th does not exhibit any substantial molecular emission. Another potential application is the remote analysis of Gd in Fukushima Daiichi Nuclear Power Station fuel debris with Fe, Ce, and Zr matrices.[43,44] Molecular LIP emission is possible due to the very distinctive GdO emission (Fig. 11).

LIBS was performed on a cerium metal sample to investigate the spectroscopic signatures and oxidation characteristics of nanosecond laser-induced plutonium surrogate plasmas. The Q-branch of the D_1-X_1 CeO transition (460-490 nm) was selected for further analysis of the plasma's oxidation behavior, as it isolates the branch head from any strong atomic transitions.[45]

CONCLUSION

The magnetic and luminescent properties of REEs make them essential components of digital and low-carbon technologies. They belong to critical elements, which are essential resources whose supply may be disrupted. Their exploration, extraction, and quantification need remote real-time analysis. LIBS principally enables such an online mode and may be suitable for the task. Nevertheless, in many cases, the traditional atomic LIBS detection of REEs is challenging due to both significant spectral interferences and the generally low concentration of REEs. With rare exceptions, the use of molecular REE emission in LIP is not even mentioned. We propose and justify the potential of such an approach.

The main areas are preliminary radiometric sorting in REE mining and electronic waste, express evaluation of the mineralogical composition and the morphological distribution of the minerals containing different REEs, in the quantification of REE in Nd–Pr–Fe-B and Sm-Co super magnets, which is required to ensure the quality of the raw material and a final product with suitable properties, in multiple applications in nuclear industry, and in analysis of one specific REE in the presence of other REE.

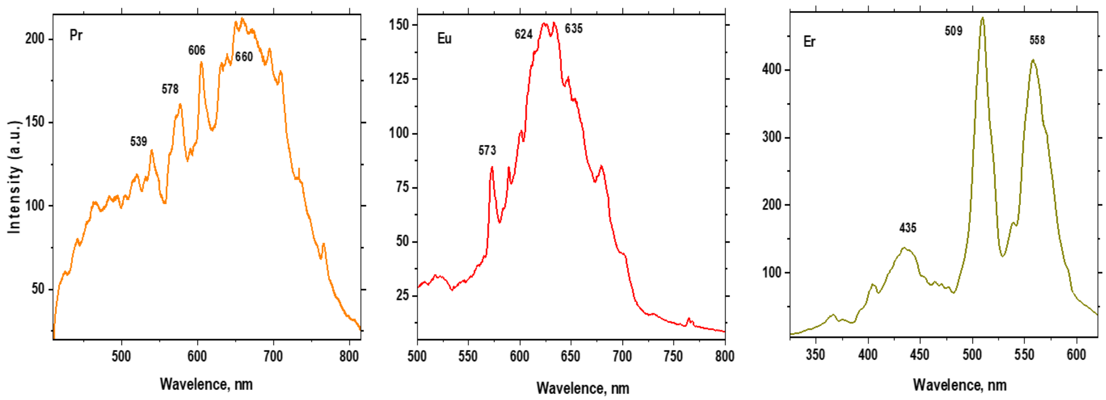

Fig. 10 Molecular emission spectra of Pr, Eu, and Er are suitable for analysis in KCl-LiCl molten salt.

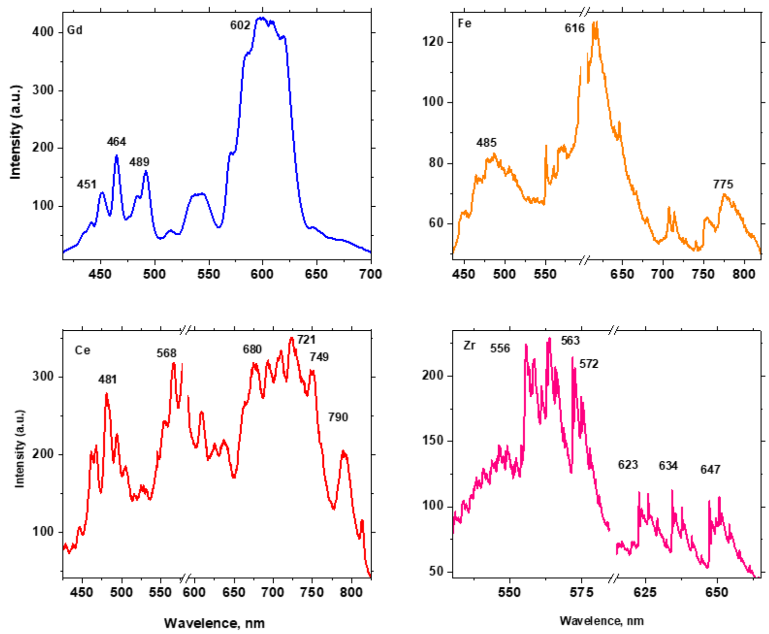

Fig. 11 Molecular emission spectra of Pr, Eu, and Er are suitable for analysis in KCl-LiCl molten salt.

AUTHOR INFORMATION

Michael Gaft received his BSc in 1975 from the Moscow Steel and Alloys Institute and PhD in 1979 from the All-Union Institute of Mineral Resources in Moscow, Soviet Union. Presently, he is an associate professor of physics at Ariel University in Israel. His primary research interests include various types of laser-induced spectroscopy, such as LIBS, Luminescence, and Raman spectroscopy, as well as their scientific and industrial applications. He emigrated to Israel in 1990 and has worked as a Physics Lecturer at the Open University of Israel, as well as serving as Chief Scientist and CEO at Laser Distance Spectrometry Company. Michael Gaft is the author or co-author of over 150 articles published in peer-reviewed scientific journals, with an h-index of 41 (Google Scholar).

Corresponding Author

* M. Gaft

E-mail address: michaelga@ariel.ac.il

Notes

The authors declare no competing financial interest.

REFERENCES

1. V. Balaram, *Geosci. Front.*, 2019, **10**, 1285−1303. https://doi.org/10.1016/j.gsf.2018.12.005
2. V. Balaram, *Minerals*, 2023, **13**, 1031. https://doi.org/10.3390/min13081031
3. A. Fayyaz, M. Aslam Baig, M. Waqas, and U. Liaqat, *Minerals*, 2024, **14**, 1004. https://doi.org/10.3390/min14101004
4. V. Mokrousov and V. Lileev, Radiometric concentration of non-radioactive ores (In Russian), Nedra, Moscow, 1979.
5. M. Gaft, R. Reisfeld, and G. Panczer, *Modern Luminescence Spectroscopy of Minerals and Materials (Second Edition), Springer*, 2015. https://link.springer.com/book/10.1007/978-3-319-24765-6
6. Ch. Robben and H. Wotruba, *Minerals*, 2019, **9**, 523. https://doi.org/10.3390/min9090523
7. D. Peukert, C. Xu, and P. Dowd, *Minerals*, 2022, **12**, 1364. https://doi.org/10.3390/min12111364
8. R. Booysen, R. Jackisch, S. Lorenz, R. Zimmermann, M. Kirsch, P.A.M. Nex, and R. Gloaguen, *Sci. Rep.*, 2020, **10**, 17450. https://doi.org/10.1038/s41598-020-74422-0
9. M. Gaft, L. Nagli, Y. Groisman, and A. Barishnikov, *Appl. Spectroc.*, 2014, **9**, 1004−1015. https://doi.org/10.1366/13-07382
10. S. Romppanen, H. Häkkänen, and S. Kaski, *Spectrochim. Acta B*, 2017, **134,** 69−74. https://doi.org/10.1016/j.sab.2017.06.002
11. C. Fabre, D. Devismes, S. Moncayo, F. Pelascini, F. Trichard, A. Lecomte, B. Bousquet, J. Cauzid, and V. Motto-Ros, *J.Anal. At. Spectrom*, 2018, **33,** 1345−1353. https://doi.org/10.1039/C8JA00048D
12. C. Fabre, *Spectrochim. Acta B*, 2020, **166**, 105799. https://doi.org/10.1016/j.sab.2020.105799
13. C. Fabre, K. Trebus, A. Tarantola, J. Cauzid, V. Motto-Ros, and P. Voudouris. *Spectrochim. Acta B*, 2022, **194,** 106470. https://doi.org/10.1016/j.sab.2022.106470
14. N. Mezoued, C. Fabre, J. Cauzid, St. Kahou, and O. Rocher, *J. Geochem. Explor.*, 2025, **271**, 107689. https://doi.org/10.1016/j.gexplo.2025.107689
15. M. Gaft, L. Nagli, A. Gorychev, and Y. Raichlin, *Spectrochim. Acta B*, 2022, **192**, 106426. https://doi.org/10.1016/j.sab.2022.106426
16. M. Sher Afgan, Z. Hou, W. Song, J. Liu, Y. Song, W. Gu, and Z. Wang, *Chemosensors*, 2022, **10**, 350. https://www.mdpi.com/2227-9040/10/9/350
17. NIST Atomic Spectra Database Lines Form. https://physics.nist.gov/PhysRefData/ASD/lines_form.html
18. S. Müller, J. A. Meima, and D. Rammlmair, *J. of Geochem. Explor*, 2021, **221**, 106697. https://doi.org/10.1016/j.gexplo.2020.106697
19. F. Xu, S. Ma, C. Zhao, and D. Dong, *Front. Phys.*, 2022, **10**, 821528. https://doi.org/10.3389/fphy.2022.821528
20. M. Gaft, L. Nagli, A. Gorychev, and Y. Raichlin, *Spectrochim. Acta B*, 2021, **182,** 0106233. https://doi.org/10.1016/j.sab.2021.106233
21. L. Nagli, M. Gaft, and Y. Raichlin, *Spectrochim. Acta B*, 2023, **202**, 10663. https://doi.org/10.1016/j.sab.2023.106631
22. M. Gaft, L. Nagli, I. Gornushkin, and Y. Raichlin, *Spectrochim. Acta B*, 2020, **173**, 105989. https://doi.org/10.1016/j.sab.2020.105989
23. M. Gaft, L. Nagli, and Y. Groisman, *Opt. Mater.*, 2011, **34**, 368−375. https://doi.org/10.1016/j.optmat.2011.05.024
24. E. Clavé, M. Gaft, V. Motto-Ros, C. Fabre, O Forni, O Beyssac, and S Maurice, *Spectrochim. Acta B*, 2021, **177**, 106111. https://doi.org/10.1016/j.sab.2021.106111
25. M. Gaft, L. Nagli, N. Eliezer, Y. Groisman, and O. Forni, *Spectrochim. Acta B*, 2014, **95**, 39−47. https://doi.org/10.1016/j.sab.2014.05.011
26. C. Fabre, L. Marulier, B. Monfaredi, V. Motto-Ros, B. Bousquet, A. Eglinger, and A. Tarantola, *Spectrochim. Acta B*, 2024, **21**, 106954. https://doi.org/10.1016/j.sab.2024.106954
27. J. Yang, Z. Liu, C. Yang, J. Gao, Z. Zhu, S. Sun, B. Hu, X. Liu, and Z. Liu, *Appl. Phys. B*, 2024, **130**, 81. https://doi.org/10.1007/s00340-024-08218-9
28. T. Ahmedganov, Determination of REE in Fe-Mn concretions by direct spectroscopic analysis. MGU, Doctoral thesis, 2024. https://papers.ssrn.com/sol3/Delivery.cfm/15404a0f-e9df-4402-85a6-d20d1ab88a0e-MECA
29. J. Yang, S. Li, Z. Zhang, D. Qian, S. Sun, X. Liu, and Z. Liu, *Talanta*, 2025, **292**, 127937. https://doi.org/10.1016/j.talanta.2025.127937
30. S. Romppane, *University of Jyväskylä*, 2021. https://jyx.jyu.fi/jyx/Record/jyx_123456789_76068
31. M. Gaft, Y. Raichlin, F. Pelascini, G. Panzer, and V. Motto Ros, *Spectrochim. Acta B*, 2019, **151**, 12−19. https://doi.org/10.1016/j.sab.2018.11.003
32. S. Imashuku, *Spectrochim. Acta A*, 2024, **315**, 124216. https://doi.org/10.1016/j.saa.2024.124216
33. L. Omodara, S. Pitkaaho, E. Turpeinen, P. Saavalainen, K. Oravisjarvi, and R. Keiski, *J. Cleaner Prod.*, 2019, **236**, 117573. https://doi.org/10.1016/j.jclepro.2019.07.048
34. C. Ramprasad, W. Gwenzi, N. Chaukura, N. Izyan Wan Azelee, A. Upamali Rajapaksha, M. Naushad, and S. Rangabhashiya, *Chem. Eng. J.*, 2022, **442**, 13599. https://doi.org/10.1016/j.cej.2022.135992
35. M. Martin, R. Fox, A. Miziolek, F. DeLucia, Jr, and N. André, *Next-Generation Spectroscopic Technologies VIII, 94820G*, 2015. https://www.researchgate.net/publication/300798048
36. J.-B. Sirven, C. Quéré, J. Maisonneuve, and B. Richebé, *Spectrochim. Acta B*, 2025, **225**, 107123. https://doi.org/10.1016/j.sab.2025.107123
37. E. Kablov, O. Ospennikova, V. Piskorskii, and I. Rezchikova, *Russian Metallurgy (Metally)*, 2015, **11**, 905−907. https://doi.org/10.1134/S0036029515110105
38. de Carvalho Elias, M. Luz, I. Gaubeur, J. Naozuka, R. Rocha, and C. Nomura, *J. Anal. At. Spectrom.*, 2023, **38,** 2105−2112. https://doi.org/10.1039/D3JA00152K
39. S. Kumar, J. Park, C. Yoo, S. Nam, and Y. Lee, *Optik*, 2021, **247**, 167919. https://doi.org/10.1016/j.ijleo.2021.167919
40. S. Kumar, J. Park, C. Yoo, S. Nam, and Y. Lee, *Anal. Methods*, 2022, **14,** 597−605. https://doi.org/10.1039/D1AY01678D
41. Y. Lee, R. Foster, H. Kim, L. Garrett, B. Morgan, M. Burger, I. Jovanovich, and S. Choi, *Anal. Chem.*, 2024, **96**, 11255−11262. https://pubs.acs.org/doi/abs/10.1021/acs.analchem.4c00897
42. X. Liu, Y. Rao, J. Liu, C. Xiong, X. Li, Y. Liu, and S. Sun, *Appl. Phys. B*, 2022, **128**, 192. https://doi.org/10.1007/s00340-022-07914-8
43. M. Batsaikhan, H. Ohba, T. Karino, K. Akaoka, and I. Wakaida, *J. Anal. At. Spectrom.*, 2024, **39,** 423−432. https://doi.org/10.1039/D3JA00347G
44. S. Almaviva, T. Karino, K. Akaoka, and I. Wakaide, *Spectrochim. Acta B*, 2024, **218**, 106960. https://doi.org/10.1016/j.sab.2024.106960
45. E. Kwapis, E. Villa-Aleman, and K. C. Hartig, *Spectrochim. Acta B*, 2023, **200**, 106610. https://doi.org/10.1016/j.sab.2022.106610